Journal of Applied Physics

RESEARCH ARTICLE | JUNE 04 2025

# Pulse train generation using a Fabry–Pérot cavity with an integrated optical amplifier and its application to parametric wavelength conversion

T. Kinoshita; S. Mine; S. Hayashi ; K. Kawase ; K. Murate



*J. Appl. Phys.* 137, 213107 (2025)
https://doi.org/10.1063/5.0261964

Journal of Applied Physics | ARTICLE | pubs.aip.org/aip/jap

# Pulse train generation using a Fabry–Pérot cavity with an integrated optical amplifier and its application to parametric wavelength conversion

Cite as: J. Appl. Phys. 137, 213107 (2025); doi: 10.1063/5.0261964
Submitted: 31 January 2025 · Accepted: 10 May 2025 ·
Published Online: 4 June 2025

View Online Export Citation CrossMark

T. Kinoshita,[1] S. Mine,[1] S. Hayashi,[2] K. Kawase,[1] and K. Murate[1,a)]

## AFFILIATIONS

[1]Department of Electronics, Nagoya University, Furocho, Nagoya 464-8603, Japan
[2]National Institute of Information and Communications Technology, Koganei, Tokyo 184-8795, Japan

[a)]**Author to whom correspondence should be addressed:** murate@nuee.nagoya-u.ac.jp

## ABSTRACT

Improving the repetition rate of a pulsed laser is an important issue in measurement and processing, as it leads to increased average power. However, in general, the heat generated by high-power lasers that use Q-switches cannot be ignored as the repetition rate increases, limiting the repetition rate. Therefore, in this study, we propose a new method of constructing a cavity in which an optical amplifier is inserted separately from the laser resonator, for generating a laser pulse train inside that cavity. By injecting a single laser pulse into this cavity, we were able to create a pulse train of up to ∼50 pulses. In addition, we confirmed that using the generated pulse train as the pump beam for a terahertz parametric source is useful to achieve a high average output. By selecting the appropriate amplifier inside the cavity, it is possible to create a pulse train from any wavelength or pulse width of the laser beam. This method makes it easier to achieve high average power from lasers when increasing the repetition rate is difficult and will contribute to the expansion of laser applications.





## I. INTRODUCTION

Pulse lasers are used in a wide range of fields, including material processing,[1] medical applications,[2] and optical measurement,[3] due to their high peak power. Increasing the repetition rate not only improves the signal-to-noise ratio of measurements and reduces processing times but also improves the average output power during wavelength conversion using nonlinear optical effects.[4–7] However, there are many technical issues involved in increasing the repetition rate of a laser system with high pulse energy. Thermal management, in particular, is a major constraint.

Currently, the most common methods for generating pulsed-laser operation are mode-locking, Q-switching, and cutting out from a semiconductor laser beam. Mode-locking technology is effective for generating short pulses and is capable of achieving extremely high repetition rates; however, the laser's output power is limited by the susceptibility of the optical elements to damage as the peak power increases. Lasers that use Q-switching can achieve high-power pulses, but the thermal effect becomes more pronounced when the repetition rate is increased, making stable operation difficult. Cutting out from a semiconductor laser beam allows modulation to any frequency, but it is difficult to achieve high output with this approach, as it is limited by the damage threshold of the device. Thus, achieving both a higher repetition rate and higher output power is a fundamental issue in laser technology.

Recent advances in power-scalable gain media have begun to bridge this energy-frequency divide. In terms of amplification methods for mode-locked lasers, chirped pulse amplification (CPA) has long played a central role. Yb:YAG CPA systems achieve both high repetition rates and high pulse energy; however, further scaling is again limited by thermal effects. To address this issue, thin-disk amplifiers and fiber amplifiers have been incorporated into the CPA systems, enabling the generation of high-output pulses at the joule level with kilohertz-order repetition rates.[8,9] In addition, alternative approaches have been proposed, such as divided-pulse amplification, in which a pulse is split into multiple sub-pulses, individually amplified, and then recombined,[10,11] as well as coherent pulse stacking, where the output of a mode-locked laser is phase-matched and stacked inside a passive enhancement cavity to increase the output power.[12]

On the other hand, achieving both high pulse energy and high repetition frequency remains challenging for single-wavelength Q-switched lasers with pulse durations longer than sub-nanoseconds. Although repetition rates on the order of 10–100 kHz have been reported using Nd:$YVO_4$ as the gain medium, the pulse energy remains on the order of 100 $\mu$J.[5,13] For higher pulse energy, devices have been developed that bond Nd:YAG, the gain medium, with sapphire, which has excellent thermal conductivity, allowing for efficient heat dissipation even under high-energy pumping conditions.[14] While the output levels in the joule class have been achieved with such devices, the repetition frequency remains limited to around 2 Hz.

Against this background, a method has been proposed to increase the repetition rate by dividing a single pulse into multiple pulses and create a pulse train by splitting the laser beam with a beam splitter and recombining it.[8–12] However, because this method divides the energy of a single pulse into multiple pulses, the energy of each pulse is the reciprocal of the number of pulses (1/number of pulses), making this approach unsuitable for increasing the average power. In this study, we attempted to install a cavity structure with an integrated amplifier, separate from the laser resonator. This configuration allows a single laser pulse to be converted into a pulse train, and the pulse energy to be maintained as the amplifier is located inside the cavity. Thus, using the proposed method, it is possible to increase the repetition rate substantially while maintaining the same high pulse energy as a Q-switched laser, which was previously difficult.

## II. PULSE TRAIN GENERATION USING A FABRY–PÉROT CAVITY

In this study, we used a Fabry–Pérot cavity[15] to create a pulse train from a laser pulse, as shown in Fig. 1. Although resonance between the two mirrors is not utilized in this setup, we refer to the system as a "cavity" for convenience. A quarter-wave plate and a polarizing beam splitter (PBS) are inserted into a cavity that is composed of two mirrors, and laser pulses enter and exit the cavity via the PBS. A laser pulse that enters the cavity travels back and forth through the quarter-wave plate and returns to the PBS. At this time, the S-polarized component (perpendicular to the figure plane) of the laser pulse is reflected by the PBS and fed back into the cavity, while the P-polarized component (parallel to the figure plane) passes through the PBS and is output from the cavity. Because the beam passes twice through the quarter-wave plate, the accumulated phase shift becomes $\pi$, effectively making it function as a half-wave plate. By rotating the quarter-wave plate, the polarization of the incident linearly polarized beam can be rotated to any desired linear polarization, and the feedback-to-output ratio can be controlled. The ratio of the laser energy incident on the cavity to the energy fed back into the cavity is referred to here as the "feedback rate." However, due to the nature of this cavity, the first pulse that is incident from the outside is P-polarized, but the second pulse and subsequent pulses are S-polarized; thus, the feedback rate takes on the exact opposite values for the first pulse and the second and subsequent pulses. It is possible to create a pulse train using this cavity; however, if there is only a waveplate in the cavity, the energy of the subsequent pulses will decrease exponentially, and the average power will not change from the initial value. Therefore, to flatten the pulse train and increase the average power, a solid-state amplifier composed of a Nd:YAG gain medium excited by three 300 W semiconductor lasers was installed inside the cavity. In this setup, the thermal lensing effect induced by the amplifier was compensated using a pair of lenses placed inside the cavity. Collimated beam was injected into the cavity, and the lens pair was adjusted so that the beam inside the cavity also remained as collimated as possible. The beam divergence was kept below approximately 0.3% per meter. The presence of a gain medium inside the cavity makes the system function similarly to a laser oscillator, leading to spontaneous oscillation caused by amplified spontaneous emission. To prevent this, a saturable absorber (Cr:YAG) was inserted into the cavity. Three types of Cr:YAG with transmittances of 30%, 60%, and 80% were used. Notably, Cr:YAG is widely employed as a saturable absorber in lasers and is considered to have sufficient long-term durability. A Faraday rotator and a polarizing beam splitter (PBS) were placed in front of the cavity to output the pulse train. The light source used was a microchip Nd:YAG laser (wavelength: 1064 nm; pulse width: 500 ps; repetition rate: 11 Hz). The cavity length was determined based on the required pulse interval. In this experiment, it was set to 6 m, which corresponds to a pulse interval of 40 ns, equivalent to a repetition rate of 25 MHz. Since the cavity was not designed to achieve



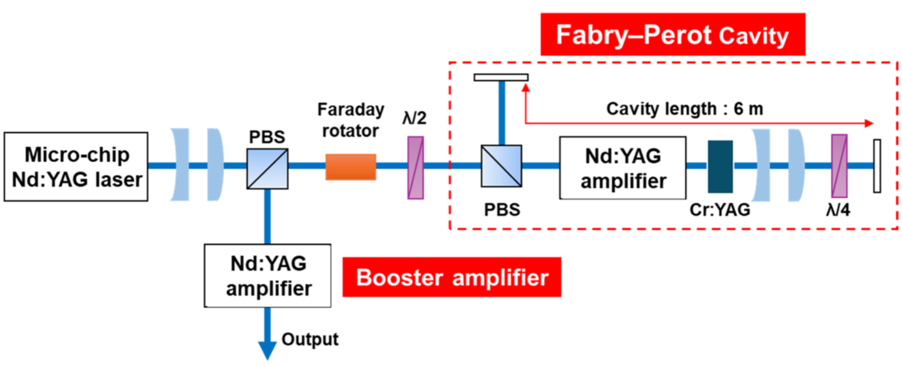


**FIG. 1.** Setup of pulse train generation.

optical resonance, neither the phase shift introduced by the wave plates nor the cavity length required strict control. Instead, the wave plates were adjusted to achieve the desired feedback ratio, and the cavity length was set to realize the target pulse interval. The laser beam reflected from the output PBS was amplified by booster amplifiers placed outside the cavity. The amplifiers were of the same type as the solid-state amplifiers used as the gain media inside the cavity and served to compensate for the energy loss caused by the insertion of Cr:YAG inside the cavity. The pulse train output generated with this configuration maintained the same single longitudinal mode as the incident beam, with a Gaussian transverse mode profile ($M^2 < 1.5$). Although an active feedback control of the cavity mirrors was not implemented in this experiment, such a control should be considered if long-term stability is required.

## III. RESULTS AND DISCUSSION

To use this configuration to create a train of laser pulses, we optimized the parameters of each element. The three values that needed to be adjusted were the Cr:YAG concentration, the feedback rate, and the amplification rate of the amplifier. The results of each measurement are shown below. The output was measured using an energy meter, and the number of pulses and the pulse train waveform were observed using a PIN photodiode.

First, we investigated the effect of the Cr:YAG concentration. The concentration of Cr:YAG and, in turn, its transmittance, affects the ease with which the cavity oscillates. To maximize the pulse energy and the number of pulses in a pulse train, it is necessary to inject external pulsed light into the amplifier while storing as much energy as possible within the amplifier. To achieve this, the power input to the amplifier must be maximized within the range where oscillation does not occur in the cavity. We, therefore, investigated the relationship between the transmittance of Cr:YAG and the oscillation threshold of the resonator (the threshold of the excitation energy of the amplifier). We compared five conditions (i)–(v): (i)–(iii) the insertion of Cr:YAG with transmittance values of 30%, 60%, or 80%, (iv) when no Cr:YAG was inserted, and (v) when all three Cr:YAG (30%, 60%, and 80%) were inserted. The oscillation threshold current increased as the transmittance of Cr:YAG decreased (Fig. 2). Although lower transmittance leads to greater attenuation of the injected pulse train, the total energy absorbed by Cr:YAG before reaching its saturation fluence—the point at which the saturable absorber becomes increasingly transparent—was still smaller than the energy that could be supplied by the amplifier under maximum pump current conditions. In other words, since the amplifier was able to deliver more energy than was lost due to absorption in Cr:YAG, the use of low-transmittance Cr:YAG was appropriate. Moreover, the presence of Cr:YAG also helps to prevent energy from concentrating into a single pulse and contributes to flattening the pulse energy distribution across the train. Based on these results, we conducted the subsequent experiments using all three Cr:YAG absorbers.

Next, we measured the effect of the feedback rate on the pulse train waveform. The current of the amplifier was set to the oscillation threshold at each feedback rate, and the transmittance of Cr:YAG was set to 14% with all three absorbers inserted. The relationship between the feedback rate to the cavity from the second pulse onward and the pulse train waveform (number of pulses, maximum pulse energy) is shown in Fig. 3(a). The actual pulse train waveforms for feedback rates of 31%, 49%, and 67% are shown in Figs. 3(b) and 3(d), respectively. The results show that lower (higher) feedback rates were associated with fewer (more) pulses and more concentrated (dispersed) energy. Ideally, both the number of pulses and the energy should increase, but there is a trade-off between the two. Therefore, it is necessary to adjust the feedback rate according to the type of the pulse train waveform required.

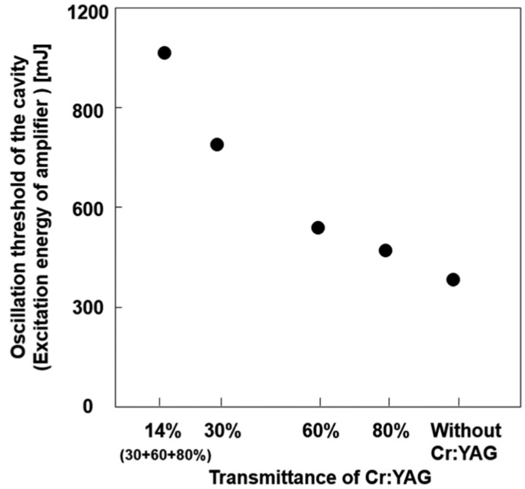


**FIG. 2.** Dependence of the cavity oscillation threshold on the transmittance of the Cr:YAG saturable absorber.

Next, we investigated the effect of the amplifier's amplification rate on the pulse train waveform. For the measurement, the cavity feedback rate was set to 49% to provide a good balance between the number of pulses and the pulse energy, and the Cr:YAG transmittance was set to 14% with all three absorbers inserted. The number of pulses and the maximum pulse energy with respect to the excitation energy of the amplifier are shown in Fig. 4(a); the actual pulse train waveforms for the excitation energy of the amplifier of 1080, 1220, and 1440 mJ are displayed in Figs. 4(b) and 4(d), respectively. The results show that the lower (higher) the amplification rate, the fewer (greater) the number of pulses and the more concentrated (dispersed) the energy. Therefore, to create the desired pulse train waveform, it is necessary to adjust the amplification rate as well as the feedback rate.

The pulse train output from the cavity was amplified further by a booster amplifier installed outside the cavity. Figure 5 shows the pulse train waveform before and after amplification by the booster amplifier. Overall, the pulse train energy was amplified; however, a much higher amplification was observed in the front pulses. We speculate that because the pulse that enters the amplifier first consumes the amplifier gain preferentially, the amplification rate is higher than that of the subsequent pulses. However, the gain and the position within the pulse train where the gain begins to

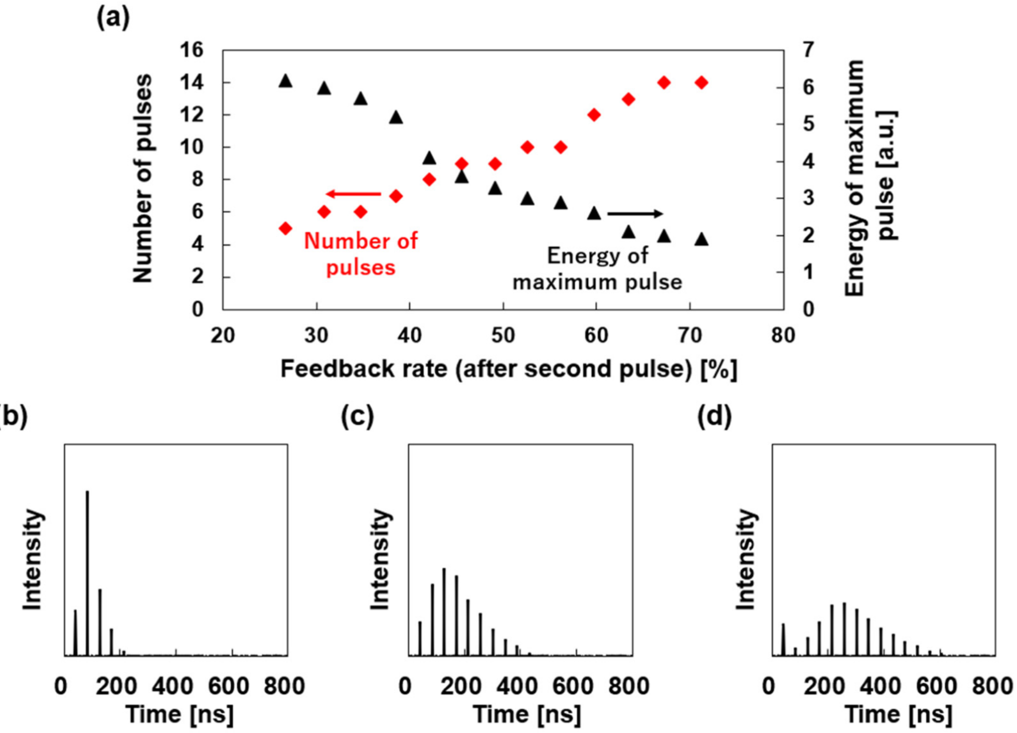


FIG. 3. (a) Dependence of the pulse train waveform on the feedback rate. Pulse train waveform at a feedback rate of (b) 31%, (c) 49%, and (d) 67%.



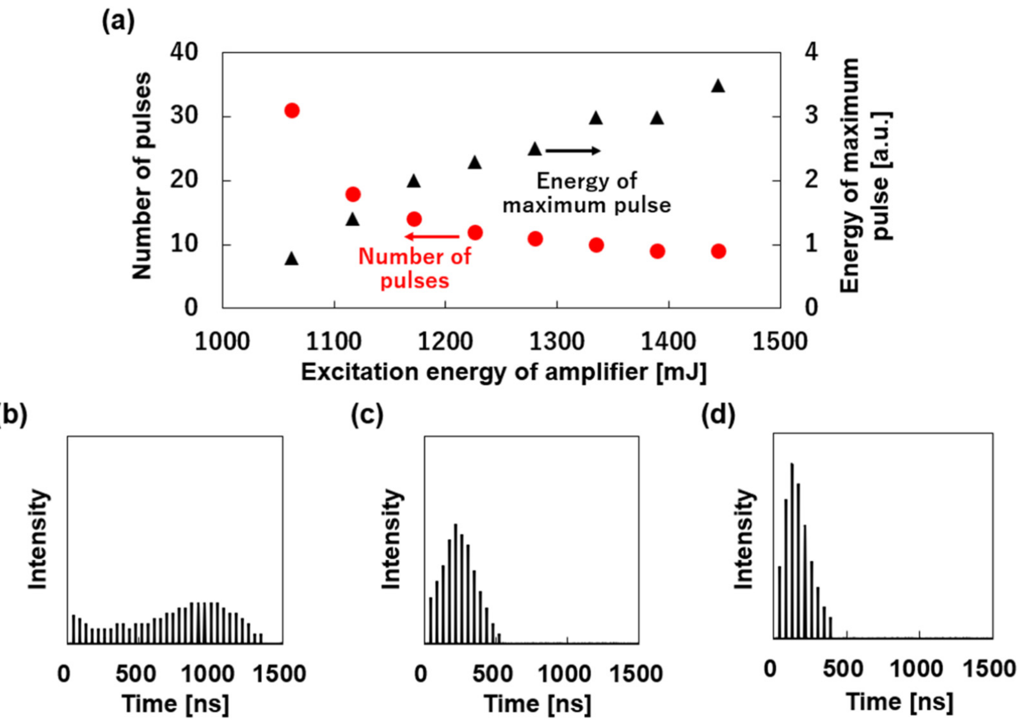


FIG. 4. (a) Dependence of the pulse train waveform on amplifier current. Pulse train waveform using an amplifier current of (b) 1080, (c) 1220, and (d) 1440 mJ.

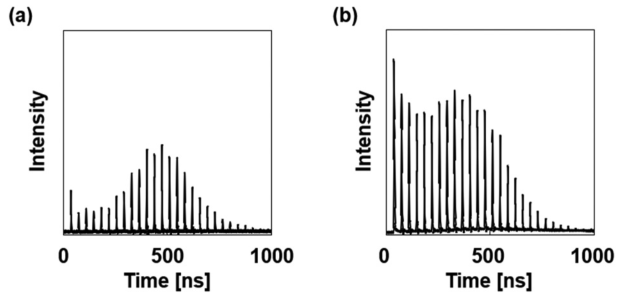


FIG. 5. Pulse train waveform (a) before and (b) after the booster amplifier.

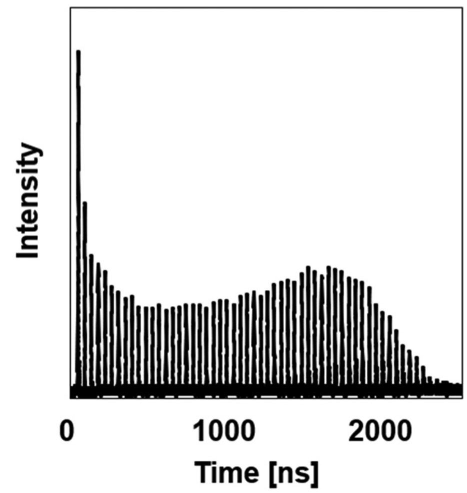


FIG. 6. The pulse train waveform generated that maximized the number of pulses (>50 pulses).

decrease depend on the input power to the booster amplifier. Therefore, when generating a pulse train, the amplification characteristics of the booster amplifier must be taken into account and the various parameters adjusted accordingly.

Figure 6 shows the pulse train waveform when the parameters of each element in the cavity and the booster amplifiers were optimized to maximize the number of pulses. The results show that a pulse train of more than 50 pulses was produced. There was bias in the pulse-energy distribution, but this was related to the feedback rate and amplifier gain. To increase the number of pulses, it is necessary to increase the feedback rate of the pulses after the second pulse; however, this is the same as decreasing the feedback rate of the first pulse so that energy is concentrated in the output component of the first pulse. The energy peaked again around the 35th pulse (Fig. 6), and the pulse energy decreased gradually. This was attributed to the depletion of the amplifier's gain and a reduction in the feedback component. In this configuration, the first pulse shows significantly higher energy, which remains a challenge to be addressed. To improve pulse flatness while securing several tens of pulses, the use of an output coupler with fixed reflectivity independent of polarization, or the insertion of a saturable absorber before the booster amplifier, could be considered.

Finally, as an application example, we introduced the pulse train of the pump beam into an injection-seeded terahertz (THz)



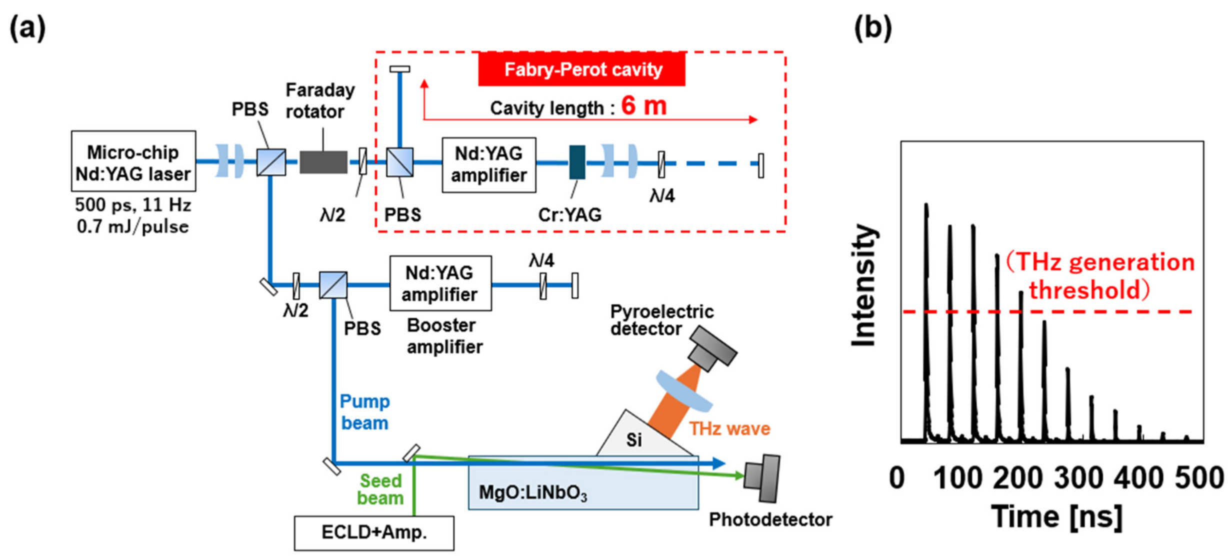


FIG. 7. (a) Setup of an injection-seeded terahertz (THz) parametric generator (is-TPG) with pulse train pump beam. (b) Pulse train pump beam used for THz-wave generation (PBS: polarizing beam splitter; ECLD: external cavity laser diode).

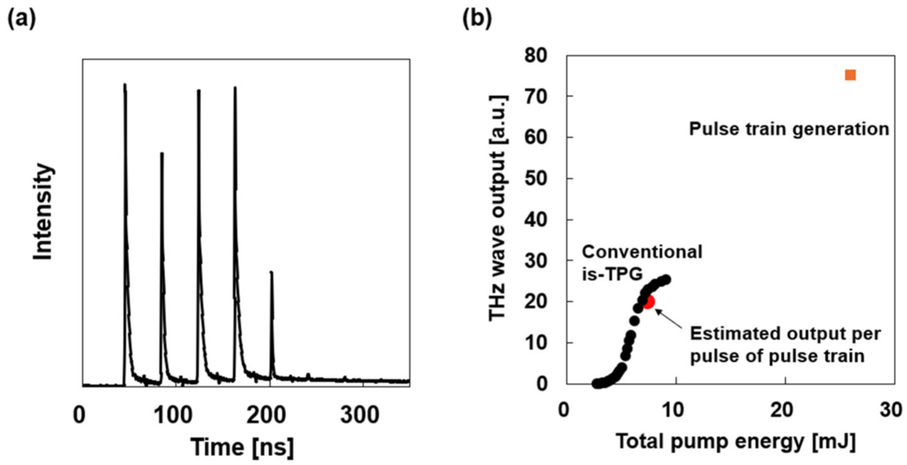


**FIG. 8.** (a) Temporal waveform of the output Stokes beam. (b) Input–output characteristics of a conventional injection-seeded terahertz (THz) parametric generator (is-TPG) and a pulse train is-TPG.

parametric generator (is-TPG).[16–19] An is-TPG is a THz-wave source with high peak power output and broadband frequency tunability that is expected to have a wide range of applications due to its ability to perform real-time spectroscopy[20,21] and to perform measurements through obstructions.[22,23] The THz waves generated by an is-TPG depend on the pump beam's intensity; however, the incident pump power is limited by the damage threshold of the MgO:$LiNbO_3$ crystal. Therefore, we increased the number of pulses while keeping the energy per pulse below the damage threshold of the crystal by making the pump beam into a train. As such, we improved the average output power of the THz waves.

The experimental setup for the is-TPG using a pulse train pump beam is shown in Fig. 7(a). The conditions required for the pump beam are as follows. First, the pulse intensity must exceed the threshold for generating THz waves. Second, each pulse must have a similar intensity. Third, the number of pulses should be as high as possible. We optimized the conditions for each of the optical elements in the cavity mentioned above and compensated for the energy loss by amplifying the energy outside the cavity. The resulting pulse train pump beam is shown in Fig. 7(b). The optimized conditions were Cr:YAG transmittance: 14%; feedback rate: 50.9%; excitation energy of the intracavity amplifier: 1330 mJ; and excitation energy of the booster amplifier: 1250 mJ.

In addition to the pump beam, an is-TPG also requires an injection seed beam. For this, we used a continuous wave laser of approximately 500 mW, which was amplified from the output of an external cavity laser diode (ECLD). THz waves were generated by injecting the pump pulse train and the seed beam into a MgO:$LiNbO_3$ crystal at an angle that satisfied the non-collinear phase-matching condition. A pyroelectric detector was used to detect the THz waves. Because a pyroelectric detector cannot acquire the temporal waveform of a THz wave, the THz-wave time waveform was approximately observed by measuring the Stokes beam (near-infrared beam) using a PIN photodiode, as the Stokes beam is generated with the THz wave as a pair in the parametric process.

Figure 8(a) shows the temporal waveform of the Stokes beam. We confirmed that the THz waves were generated by all five pulses that exceeded the generation threshold, as shown in Fig. 7(b). The Stokes beam intensity decreased only for the fifth pulse because the pump energy was small. The results of comparing the THz-wave output of a conventional is-TPG with that of the pulse train is-TPG are shown in Fig. 8(b). The black dots represent the measured THz-wave output of the conventional is-TPG as a function of input pump power, while the orange dots indicate the total THz-wave output generated by the pulse train. The red dots show the estimated THz-wave output per pulse, calculated by dividing the total output of the pulse train by the number of pulses. Comparing the per-pulse THz-wave output of the pulse train is-TPG (red dots) with that of the conventional is-TPG (black dots), we find that the efficiency of the two approaches is nearly the same, and that the total output increases proportionally with the number of pulses. This implies that by further increasing the number of pulses, it would be possible to obtain a THz-wave output with higher average power while maintaining sufficient pulse energy, thus demonstrating the usefulness of a pulse train pump beam for achieving a high average output from an is-TPG.



## IV. CONCLUSION

In this study, we sought to increase both the pulse energy and the repetition rate, which can be difficult to achieve simultaneously in a pulsed laser. It is generally difficult to increase the repetition rate of lasers with high pulse energy, such as Nd:YAG lasers, due to thermal effects. Therefore, we installed a laser cavity containing an amplifier outside the laser to create a pulse train. By optimizing the Cr:YAG transmittance, the feedback rate, and the amplification rate, we created a pulse train with a maximum of >50 pulses. When this pump pulse train was applied to an is-TPG to generate THz waves, an improvement in average power was observed compared to that provided by a conventional is-TPG configuration, demonstrating the usefulness of the pulse train pump beam. This method can be applied to generate pulse trains from a laser pulse of various wavelengths and pulse widths, not only 1064 nm, by selecting an appropriate amplifier in the cavity. Thus, this approach enables high average power in laser systems in which it was previously difficult to increase the repetition rate; further applications are expected.

## ACKNOWLEDGMENTS

The authors appreciate the fruitful discussions with Dr. Y. Urata from PHLUXi, Inc., and Dr. K. Takeya from Institute for Molecular Science. This work was partially supported by Japan Science and Technology Agency (JST) Adopting Sustainable Partnerships for Innovative Research Ecosystem Program (No. JPMJAP2340) and FOREST Program (No. JPMJFR212J) and Japan Society for the Promotion of Science KAKENHI (Nos. 22J20963 and 24K00943).

## AUTHOR DECLARATIONS

### Conflict of Interest

The authors have no conflicts to disclose.

### Author Contributions

**T. Kinoshita:** Data curation (lead); Formal analysis (lead); Methodology (equal); Resources (equal); Validation (equal); Visualization (lead); Writing – original draft (lead). **S. Mine:** Formal analysis (supporting); Methodology (supporting); Resources (supporting); Validation (supporting); Writing – original draft (supporting); Writing – review & editing (supporting). **S. Hayashi:** Conceptualization (equal); Methodology (equal); Writing – review & editing (supporting). **K. Kawase:** Funding acquisition (supporting); Validation (supporting); Writing – review & editing (equal). **K. Murate:** Conceptualization (lead); Data curation (supporting); Funding acquisition (lead); Investigation (supporting); Methodology (lead); Project administration (lead); Supervision (lead); Validation (supporting); Visualization (supporting); Writing – original draft (supporting); Writing – review & editing (lead).

## DATA AVAILABILITY

The data that support the findings of this study are available from the corresponding author upon reasonable request.

## REFERENCES

[1]G. Račiukaitis, "Ultra-short pulse lasers for microfabrication: A review," IEEE J. Sel. Top. Quantum Electron. **27**(6), 1–12 (2021).

[2]A. Vogel, and V. Venugopalan, "Mechanisms of pulsed laser ablation of biological tissues," Chem. Rev. **103**(2), 577–644 (2003).

[3]I. Coddington, W. C. Swann, L. Nenadovic, and N. R. Newbury, "Rapid and precise absolute distance measurements at long range," Nat. Photonics **3**(6), 351–356 (2009).

[4]B. Green, S. Kovalev, V. Asgekar, G. Geloni, U. Lehnert, T. Golz, M. Kuntzsch, C. Bauer, J. Hauser, J. Voigtlaender, B. Wustmann, I. Koesterke, M. Schwarz, M. Freitag, A. Arnold, J. Teichert, M. Justus, W. Seidel, C. Ilgner, N. Awari, D. Nicoletti, S. Kaiser, Y. Laplace, S. Rajasekaran, L. Zhang, S. Winnerl, H. Schneider, G. Schay, I. Lorincz, A. A. Rauscher, I. Radu, S. Mährlein, T. H. Kim, J. S. Lee, T. Kampfrath, S. Wall, J. Heberle, A. Malnasi-Csizmadia, A. Steiger, A. S. Müller, M. Helm, U. Schramm, T. Cowan, P. Michel, A. Cavalleri, A. S. Fisher, N. Stojanovic, and M. Gensch, "High-field high-repetition-rate sources for the coherent THz control of matter," Sci. Rep. **6**(1), 22256 (2016).

[5]Y. Moriguchi, Y. Tokizane, Y. Takida, K. Nawata, T. Eno, S. Nagano, and H. Minamide, "High-average and high-peak output-power terahertz-wave generation by optical parametric down-conversion in MgO:$LiNbO_3$," Appl. Phys. Lett. **113**(12), 121103 (2018).

[6]Y. Yang, G. Zhao, Y. Huang, L. Feng, S. Huang, and K. Liu, "High repetition rate picosecond $LiNbO_3$ THz parametric amplifier and parametric gain," Chin. Opt. Lett. **18**(5), 051901 (2020).

[7]K. Ravi, D. N. Schimpf, and F. X. Kärtner, "Pulse sequences for efficient multi-cycle terahertz generation in periodically poled lithium niobate," Opt. Express **24**(22), 25582–25607 (2016).

[8]T. Nubbemeyer, M. Kaumanns, M. Ueffing, M. Gorjan, A. Alismail, H. Fattahi, J. Brons, O. Pronin, H.G. Barros, Z. Major, T. Metzger, D. Sutter, and F. Krausz, "1 kW, 200 mJ picosecond thin-disk laser system," Opt. Lett. **42**(7), 1381–1384 (2017).

[9]Y. Wang, H. Chi, C. Baumgarten, K. Dehne, A.R. Meadows, A. Davenport, G. Murray, B.A. Reagan, C.S. Menoni, and J. J. Rocca, "1.1 J Yb:YAG picosecond laser at 1 kHz repetition rate," Opt. Lett. **45**(24), 6615–6618 (2020).

[10]B. Webb, A. Azim, N. Bodnar, M. Chini, L. Shah, and M. Richardson, "Divided-pulse amplification to the joule level," Opt. Lett. **41**(13), 3106–3109 (2016).

[11]Z. Shi, J. Wang, Y. Zhang, J. Wang, Z. Wei, and G. Chang, "Generation of 107 W, 1.07 mJ femtosecond pulses from chirped- and divided-pulse Sagnac Yb-fiber amplifiers by suppression of static mode degradation," JOSA B **40**(9), 2429–2433 (2023).

[12]S. Breitkopf, T. Eidam, A. Klenke, L. von Grafenstein, H. Carstens, S. Holzberger, E. Fill, T. Schreiber, F. Krausz, A. Tünnermann, I. Pupeza, and J. Limpert, "A concept for multiterawatt fibre lasers based on coherent pulse stacking in passive cavities," Light Sci. Appl. **3**(10), e211 (2014).

[13]C. Wang, C. Liu, L. Shen, Z. Zhao, B. Liu, and H. Jiang, "1.6 MW peak power, 90 ps all-solid-state laser from an aberration self-compensated double-passing end-pumped Nd:$YVO_4$ rod amplifier," Appl. Opt. **55**(9), 2399–2403 (2016).

[14]V. Yahia, A. Kausas, A. Tsuji, M. Yoshida, and T. Taira, "Joule-class sub-nanosecond pulses produced by end-pumped direct bonded YAG/sapphire modular amplifier," Opt. Express **32**(8), 14377–14393 (2024).

[15]G. Hernandez, *Fabry-Perot Interferometers* (Cambridge University Press, 1988).

[16]K. Murate, and K. Kawase, "Perspective: Terahertz wave parametric generator and its applications," J. Appl. Phys. **124**(16), 160901 (2018).

[17]S. Hayashi, K. Nawata, T. Taira, J. Shikata, K. Kawase, and H. Minamide, "Ultrabright continuously tunable terahertz-wave generation at room temperature," Sci. Rep. **4**(1), 5045 (2014).

[18]K. Nawata, S. Hayashi, H. Ishizuki, K. Murate, K. Imayama, Y. Takida, V. Yahia, T. Taira, K. Kawase, and H. Minamide, "Effective terahertz wave parametric generation depending on the pump pulse width using a $LiNbO_3$ crystal," IEEE Trans. Terahertz Sci. Technol. **7**(5), 617–620 (2017).

[19]K. Chen, L. Tang, D. Xu, Y. Wang, C. Yan, G. Nie, C. Hu, B. Wu, J. Zhu, and J. Yao, "Continuously tunable and energy-enhanced injection pulse-seeded terahertz parametric generator based on KTP crystal," ACS Photonics **8**(11), 3141–3149 (2021).

[20]K. Murate, S. Mine, Y. Torii, H. Inoue, and K. Kawase, "Wide dynamic range and real-time reagent identification and imaging using multi-wavelength terahertz parametric generation and machine learning," Sci. Rep. **13**(1), 12743 (2023).

[21]K. Murate, R. Kawaguchi, S. Hayashi, and K. Kawase, "Pulse burst multiwavelength terahertz-wave spectroscopic measurement using parametric wavelength conversion," IEEE Trans. Terahertz Sci. Technol. **13**(5), 561–564 (2023).

[22]R. Mitsuhashi, K. Murate, S. Niijima, T. Horiuchi, and K. Kawase, "Terahertz tag identifiable through shielding materials using machine learning," Opt. Express **28**(3), 3517–3527 (2020).

[23]K. Murate, S. Mine, and K. Kawase, "Terahertz parametric generators and detectors for nondestructive testing through high-attenuation packaging materials," IEEE J. Sel. Top. Quantum Electron. **29**(5), 1–13 (2023).